New Routes to Studying the Dressed Photon

M. Ohtsu[1,2]

[1] Institute of Engineering Innovation, Graduate School of Engineering,
The University of Tokyo, 2-11-16 Yayoi, Bunkyo-ku, Tokyo, 113-8656, Japan

[2] Research Origin for Dressed Photon, c/o the University of Tokyo,
Bdg. Eng-9, 2-11-16 Yayoi, Bunkyo-ku, Tokyo, 113-8656, Japan

Abstract: First, this paper reviews the history of studies on the dressed photon (DP) by classifying them into older and modern times, between which there exists a great difference in the concepts, principles, and methods involved. Quantum field theories, developed more recently, have succeeded in solving three problems originating from the intrinsic features of the light–matter interactions occurring in nanometric spaces. First, a variety of applications of these theoretical studies, which have resulted in the development of generic technology, are introduced. Second, the present status of experimental studies is reviewed. Among them, the fabrication and operation of novel light emitting devices using crystalline silicon (Si) are demonstrated. In these devices, the DP enabled high-power light emission even though Si is an indirect-transition-type semiconductor. Furthermore, it is shown that these devices exhibit a unique feature, named photon breeding. Third, a future outlook of DP research is presented, where it is pointed out that novel theoretical studies are required in order to support the rapid progress made in recent experimental studies and to develop further novel application technologies. As a route to such novel theoretical studies, three steps are presented, and several results derived from these steps are reviewed. Furthermore, a theory of micro–macro duality in the quantum field is presented as a powerful tool that will enable future progress in theoretical studies. Finally, a variety of phenomena in nano-systems, macro-systems, inorganic materials, and organic materials, which have similar features to those of the DP, are introduced. By referring to this similarity, it is pointed out that studies on the DP are connected to a more generic and broader science that is expected to produce a novel generic science, named off-shell science, in the near future.

1 Introduction

The dressed photon (DP), a novel form of photon created in a nanometer-sized space, has been referred to as an optical near field, and the science for dealing with this type of photon has been called near field optics. The history of near field optics is long and can be classified into older and modern times, based on the great differences in the concepts, principles, and methods of studying the DP. The older time started with a simple proposal to use light falling on a sub-wavelength sized aperture for high-resolution microscopy [1]. After a long time during which this proposal was ignored, theoretical analyses were carried out on the diffraction and radiation of electromagnetic waves through a small aperture [2,3]. Afterward, these analyses were experimentally demonstrated by using microwaves [4].

Demonstrations using light were finally carried out using a novel methodology, named near-field optical microscopy, by several scientists in several countries, including Japan (M.O.), almost simultaneously [5]. Among them, this author (M.O.) developed high-quality optical fiber probes for generating and detecting optical near fields with high resolution and high sensitivity (Fig. 1) [6]. These fiber probes have been used to assemble novel spectrometers, and microscopic and spectroscopic images of specimens, e.g., a single strand of DNA, were successfully acquired with a high resolution beyond the diffraction limit [7]. They have since become commercially available and have been exported to many countries around the world [8].

Based on the successful experimental demonstrations above, the Near-Field Optics Workshop has held in order to promote basic studies and applications of optical near fields [5]. In this workshop, a physical picture of the optical near field was drawn using a conventional optical method, i.e., by using the dispersion relation between the momentum and energy of the photon. After this workshop, the International Near-Field Optics Conference was organized, and the most recent 14th conference was held in 2016 [9]. In order to promote near field optics in the Asia-Pacific area, the author organized the Asia-Pacific Workshop on Near-Field Optics in 1996 [10]. After this workshop, the Asia-Pacific Near-Field Optics Conference was also organized, and the most recent 11th conference was held in 2017 [11].

It should be pointed out that the older time mentioned above has already ended. The reason for this is that conventional optical microscopy is

based on the methodology of nondestructive measurement of the specimen's conformation and/or structure, which is described by conventional optics. Unlike this conventional microscopy, near-field optical microscopy is based on destructive measurement because it acquires an image of the specimen through optical near field interactions between the probe tip and the specimen. Even though a high resolution beyond the diffraction limit of light could be realized by this microscopy, a fatal problem was that electronic energy levels in the specimen were disturbed as a result of these interactions, which resulted in the acquired image profile being different from and uncorrelated with the conventional optical microscope images.

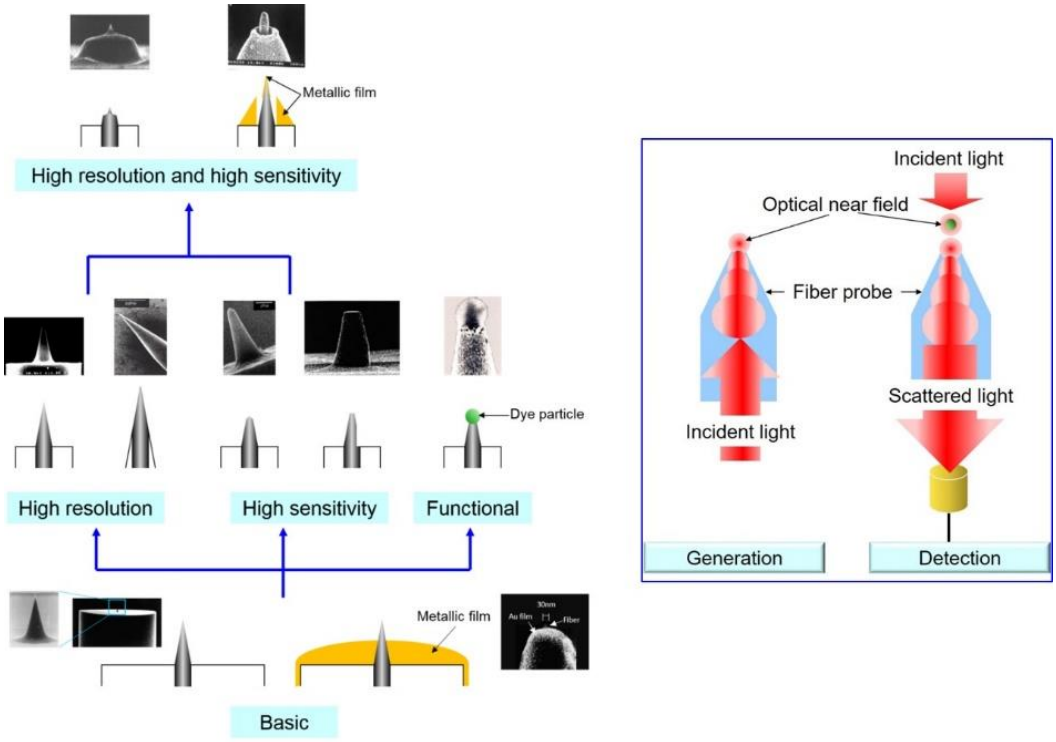

Fig. 1 High-quality fiber probes.

Noting this difference, the application of the optical near field to microscopy ended, and the modern time started. In the modern time, enormous efforts were devoted to studying the above-mentioned optical near field interactions, i.e., light–matter interactions that take place via the optical near field.

This paper reviews a brief history of the modern time and describes the present status of studies on the DP [12]. A future outlook on theoretical

studies is also presented, followed by some concluding remarks.

2 History of the modern time

As was pointed out in the previous section, there were great differences between studies on the DP in the older and modern times in terms of their concepts, principles, and methods. That is, the studies promoted in the modern time are essentially incompatible with those in the older time. They are called off-shell and on-shell sciences, respectively, as will be reviewed in Section 4. In the modern time, extensive experimental studies were carried out by using two kinds of materials. The first kind was metals, in which plasmonic oscillation of the free electrons was utilized. Although the ease of fabricating nanometer-sized metallic particles or metallic thin films was high, these materials had two intrinsic features; a short conversion time from the optical energy to the plasmonic oscillation energy of the electrons, and a short phase-relaxation time of the electrons. Due to these short time constants, the quantum nature of the incident light was not maintained in the metal. Therefore, quantum field theory was not required for describing the light–matter interactions in the metal,; instead, the conventional optical theory was sufficient, and conventional parameters, including the optical refractive index, the wave-number, and the mode, were used. This means that the dispersion relation was valid for describing the interactions, as has been used since the Near-Field Optics Workshop a quarter of a century ago. This situation means that studies using the first kind of material were left behind by the modern time.

Productive experimental studies in the modern time were promoted by using the second kind of materials, including semiconductors, organic materials, and gaseous molecules, in which their discrete electronic energy levels were utilized. Although fabrication of nanometer-sized particles or thin films was not straightforward in the beginning, technological advances enabled fabrication of suitable devices, which promoted further studies. As a result, a variety of applications were developed to establish a generic technology, as illustrated in Fig. 2 [13]. They include: lithography [14] and information storage [15] at densities beyond the diffraction limit, polishing of material surfaces to atomic-level flatness [16], photon breeding devices [17], logic gate devices [18], optical router systems [19], optical pulse shape

measurement systems [20], optical security systems [21], energy conversion systems [22,23], and so on.

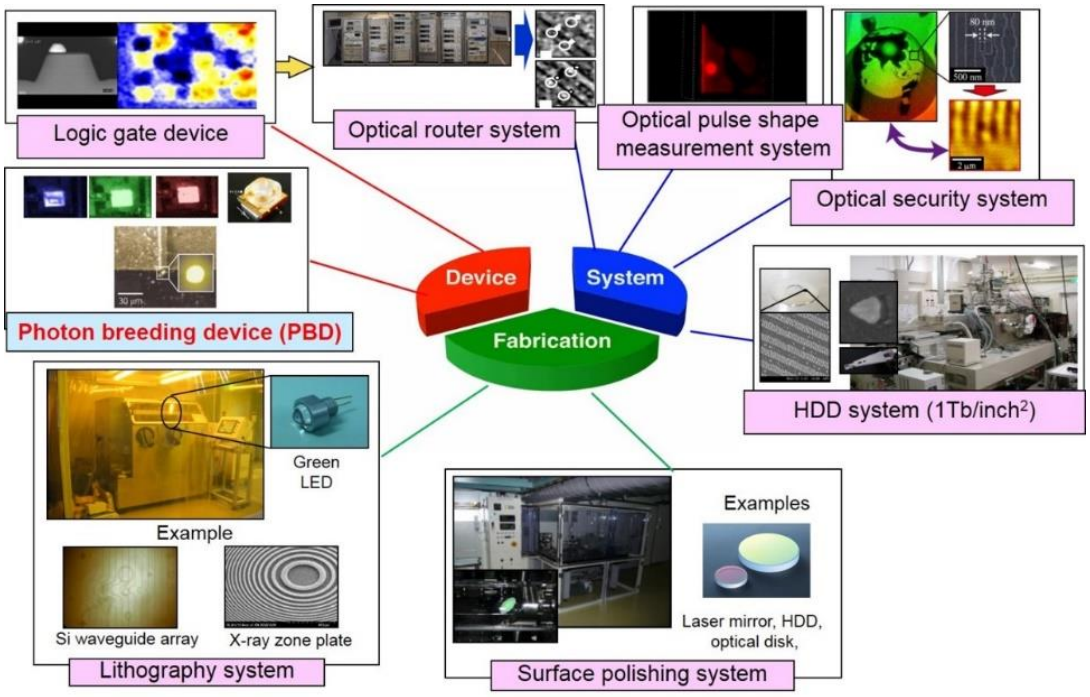

Fig. 2 A variety of applications.

To promote experimental studies in the modern time, three theoretical problems had to be solved:

[1] **Problem 1**: Quantum field theory for photons and electron–hole pairs was required to describe the light–matter interactions taking place in a nanometric space. However, the problem was that a virtual cavity, for deriving the Hamiltonian operator, could not be defined because the sub-wavelength-sized optical near field existed in a nanometric space. In other words, the electromagnetic mode could not be defined. It should be noted that the optical near field was regarded neither as a collection of corpuscles nor as a free photon, proposed by Newton and Einstein, respectively.

To solve this problem, a novel physical picture of the optical near field was drawn by representing the Hamiltonian operator $\hat{H}$ under illumination with propagating light having photon energy $\hbar w_o$:

$$\hat{H} = \sum_{\mathbf{k}\lambda} \hbar\omega_{\mathbf{k}} \hat{a}^{\dagger}_{\mathbf{k}\lambda} \hat{a}_{\mathbf{k}\lambda} + \sum_{\alpha>F,\beta<F} \left(E_{\alpha} - E_{\beta}\right) \hat{b}^{\dagger}_{\alpha\beta} \hat{b}_{\alpha\beta} + \hat{H}_{\text{int}} . \qquad (1)$$

The first term represents the photon energy created in the nanometric space,

which is given by the sum of an infinite number of photon modes with angular frequency $\omega_{\boldsymbol{k}}$, polarization state λ, and energy $\hbar\omega_{\boldsymbol{k}}$. Here, the subscript $\boldsymbol{k}$ represents the wave-vector, and $\hat{a}_{\boldsymbol{k}\lambda}$ and $\hat{a}^{\dagger}_{\boldsymbol{k}\lambda}$ are annihilation and creation operators, respectively. They satisfy the commutation relation

$$\left[\hat{a}_{\boldsymbol{k}\lambda}, \hat{a}^{\dagger}_{\boldsymbol{k}'\lambda'}\right] = \delta_{\boldsymbol{k}\boldsymbol{k}'}\delta_{\lambda\lambda'}, \tag{2}$$

where $\delta_{\boldsymbol{k}\boldsymbol{k}'}$ and $\delta_{\lambda\lambda'}$ are Kronecker deltas. The second term represents the energy of the electron–hole pair, which is also given by the sum of the energies of the electron–hole pairs of the infinite number of energy levels, identified by the subscripts a and b. The energy difference E_a - E_b represents the bandgap energy in the case of a semiconductor, and F represents the Fermi energy level. The operators $\hat{b}_{\alpha\beta}$ and $\hat{b}^{\dagger}_{\alpha\beta}$ respectively represent the simultaneous annihilation and creation of the electron and hole, i.e., the annihilation and creation operators of the electron–hole pair. They satisfy the commutation relation

$$\left[\hat{b}_{\alpha\beta}, \hat{b}^{\dagger}_{\alpha'\beta'}\right] = \delta_{\alpha\alpha'}\delta_{\beta\beta'}. \tag{3}$$

The third term represents the energy of the interaction between the photon and the electron–hole pair, which is given by

$$\hat{H}_{\mathrm{int}} = -\int \hat{\psi}^{\dagger}(\boldsymbol{r})\,\boldsymbol{p}(\boldsymbol{r})\hat{\psi}(\boldsymbol{r})\cdot\hat{\boldsymbol{D}}^{\perp}(\boldsymbol{r})\,dv, \tag{4}$$

where $\boldsymbol{p}(\boldsymbol{r})$ is an electric dipole moment, $\hat{\psi}(\boldsymbol{r})$ and $\hat{\psi}^{\dagger}(\boldsymbol{r})$ are respectively annihilation and creation operators for the field of the electron–hole pair, and $\hat{\boldsymbol{D}}^{\perp}(\boldsymbol{r})$ is the transverse component of the electric displacement operator of the incident propagating light, which is perpendicular to the wave-vector $\boldsymbol{k}$. This operator $\hat{\boldsymbol{D}}^{\perp}(\boldsymbol{r})$ is expressed as

$$\hat{\boldsymbol{D}}^{\perp}(\boldsymbol{r}) = i\sum_{\boldsymbol{k}}\sum_{\lambda=1}^{2} N_{\boldsymbol{k}}\boldsymbol{e}_{\boldsymbol{k}\lambda}(\boldsymbol{k})\left\{\hat{a}_{\boldsymbol{k}\lambda}(\boldsymbol{k})e^{i\boldsymbol{k}\cdot\boldsymbol{r}} - \hat{a}^{\dagger}_{\boldsymbol{k}\lambda}(\boldsymbol{k})e^{i\boldsymbol{k}\cdot\boldsymbol{r}}\right\}, \tag{5}$$

where plane waves are used for the mode functions. Here, $N_{\boldsymbol{k}}$ and $\boldsymbol{e}_{\boldsymbol{k}\lambda}(\boldsymbol{k})$ are a proportionality constant and the unit vector along the direction of polarization, respectively.

By diagonalizing the Hamiltonian operator of eq. (1), annihilation and creation operators ($\tilde{a}$ and $\tilde{a}^{\dagger}$, respectively) of the novel quasi-particle were derived, which represented the quantum state of the coupled photon and electron–hole pairs as a result of their interaction in the nanometric space:

$$\tilde{a} = \sum_{\boldsymbol{k}\lambda} \left\{ \hat{a}_{\boldsymbol{k}\lambda} - iN_{\boldsymbol{k}} \sum_{\alpha>F,\beta<F} \left(\rho^{*}_{\alpha\beta\lambda}(\boldsymbol{k}) \hat{b}_{\alpha\beta} + \rho^{*}_{\beta\alpha\lambda}(\boldsymbol{k}) b^{\dagger}_{\alpha\beta} \right) \right\}, \tag{6}$$

and

$$\tilde{a}^{\dagger} = \sum_{\boldsymbol{k}\lambda} \left\{ \hat{a}^{\dagger}_{\boldsymbol{k}\lambda} + iN_{\boldsymbol{k}} \sum_{\alpha>F,\beta<F} \left(\rho_{\alpha\beta\lambda}(\boldsymbol{k}) \hat{b}^{\dagger}_{\alpha\beta} + \rho_{\beta\alpha\lambda}(\boldsymbol{k}) b_{\alpha\beta} \right) \right\}, \tag{7}$$

where $\rho_{\alpha\beta\lambda}(\boldsymbol{k})$ is the spatial Fourier transform of the electric dipole moment. These operators are represented by the sum of the operators for the photons of the infinite number of modes and for the electron–hole pairs of the infinite number of energy levels. Because of this summation, this quasi-particle was named the dressed photon (DP), i.e., a photon dressed by the material excitation energy (Fig. 3)[24].

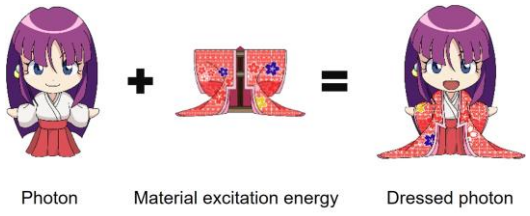

Fig.3 Illustrative explanation of the dressed photon.

[2] Problem 2: Since the DP is non-propagating and localized on a nanomaterial, another nanomaterial was required for its detection; in other words, another material had to be placed in close proximity to convert the DP to propagating light via multiple scattering of the DP. Here, the problem was

how to describe this scattering, because the two nanomaterials, i.e., the source and detector for the DP, are not independent of each other but are coupled via the DP. However, this problem was solved by using the solution to problem 1. That is, scattering was described by using the annihilation and creation operators of DPs on the two nanomaterials.

[3] Problem 3: Since the actual nanomaterials and DP are always surrounded by a macroscopic system composed of macroscopic materials and macroscopic optical fields, the problem was how to take into account the contribution from the macroscopic energy in order to derive the magnitude of the DP interaction energy between nanomaterials. To solve this problem, the contributions from the macroscopic system were renormalized by the projection operator method. As a result, the magnitude of the DP interaction energy was derived and represented by a Yukawa function:

$$Y(r) = \frac{\exp(-r/a)}{r}, \tag{8}$$

where r is the distance from the center of the nanomaterial, and a represents the extent of localization, which is equivalent to the size of the nanomaterial [25].

In the solution to problem 3 above, it should be noted that a is independent of the wavelength λ of the incident propagating light. Furthermore, the DP is strongly localized in the sub-wavelength-sized space because $a \ll \lambda$. Due to this localization, the following two novel phenomena were found: The first one is with respect to the electronic transition. For explaining this transition, an atom with a simple two-energy level electron is considered by assuming that the state functions of these levels have the same parity. In this case, the electric dipole transition is forbidden under irradiation with propagating light incident on the atom. This is because the state functions have the same parity and, more essentially, the long-wavelength approximation is valid. However, this electric dipole-forbidden transition turns out be allowed in the case where the DP is involved. This is because the long-wavelength approximation is not valid any more since $a \ll \lambda$. The second phenomenon was named size-dependent resonance; in this phenomenon, the magnitude of the DP energy transferred between the two nanomaterials takes a maximum when the sizes of these

nanomaterials are equal [26]. This corresponds to the momentum conservation law for the DP. It is different from diffraction, which is a typical phenomenon in classical optics, where the cross-sectional size of the light beam on a screen after being transmitted through an aperture is inversely proportional to the aperture size. By utilizing these two phenomena, a variety of applications were developed, some of which are shown in Fig. 2. To realize more developments, further theoretical studies were carried out.

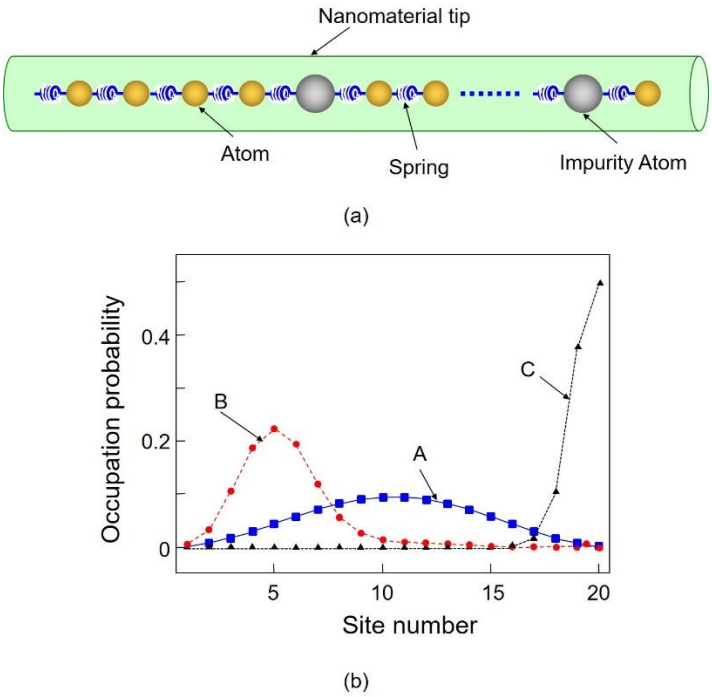

Fig. 4 Occupation probability of the dressed photon.

(a) One-dimensional model for calculation. The number of atoms is 20. The impurity atoms are at sites 4, 6, 13, and 19. (b) Calculated results. The mass of the impurity atoms is 0.2-times that of the other atoms. $\hbar\omega = 1.81$ eV and $\hbar J = 0.5$ eV. Curves A, B, and C represent the results for $\chi = 0$, 40.0, and 54.0 $fs^{-1}nm^{-1}$, respectively.

One successful result of these studies was the further possibility of dressing, i.e., the possibility of coupling DPs and phonons [27]. In order to describe this coupling, for simplicity a nanomaterial tip is assumed, in which a one-dimensional crystal lattice is provided (Fig. 4(a)). When the tip is illuminated with light, a DP can be created on a lattice site and hops to an adjacent site. During the hopping, the DP can excite lattice vibrations to create phonons, and then the DP couples with these phonons.

For a theoretical formulation of this coupling, the Hamiltonian

operator $\hat{H}$ is given by

$$\hat{H} = \sum_{i=1}^{N} \hbar\omega \tilde{a}_i^{\dagger} \tilde{a}_i + \sum_{p=1}^{N} \hbar\Omega_p \hat{c}_p^{\dagger} \hat{c}_p + \sum_{i=1}^{N} \sum_{p=1}^{N} \hbar\chi_{ip} \tilde{a}_i^{\dagger} \tilde{a}_i \left(\hat{c}_p^{\dagger} + \hat{c}_p \right) + \sum_{i=1}^{N-1} \hbar J \left(\tilde{a}_i^{\dagger} \tilde{a}_{i+1} + \tilde{a}_{i+1}^{\dagger} \tilde{a}_i \right). \tag{9}$$

In the first term, $\tilde{a}_i$ and $\tilde{a}_i^{\dagger}$ respectively denote the annihilation and creation operators of a DP with energy $\hbar w$ at site i in the lattice. In the second term, $\hat{c}_p$ and $\hat{c}_p^{\dagger}$ are respectively the annihilation and creation operators of the phonon of mode p, which satisfies the boson commutation relation:

$$\left[\hat{c}_p, \hat{c}_q^{\dagger} \right] \equiv \hat{c}_p \hat{c}_q^{\dagger} - \hat{c}_q^{\dagger} \hat{c}_p = \delta_{pq}. \tag{10}$$

The phonon energy is represented by $\hbar\Omega_p$. The third and fourth terms stand for the DP–phonon interaction with the interaction energy $\hbar\chi_{ip}$ and DP hopping with hopping energy $\hbar J$, respectively.

By diagonalizing $\hat{H}$ of eq. (9), annihilation and creation operators of the novel quasi-particle are derived and expressed as

$$\hat{\alpha}_i = \tilde{a}_i \exp\left\{ \sum_{p=1}^{N} \frac{\chi_{ip}}{\Omega_p} \left(\hat{c}_p^{\dagger} - \hat{c}_p \right) \right\}, \tag{11}$$

$$\hat{\alpha}_i^{\dagger} = \tilde{a}_i^{\dagger} \exp\left\{ -\sum_{p=1}^{N} \frac{\chi_{ip}}{\Omega_p} \left(\hat{c}_p^{\dagger} - \hat{c}_p \right) \right\}, \tag{12}$$

which is the product of the DP operator of eqs. (6) and (7) and the displacement operator function for the phonon. It should be noted that this function creates a multi-mode phonon with a coherent state. In other words, the DP excites a multi-mode coherent phonon, and they coupled to form a novel quasi-particle named a dressed-photon–phonon (DPP). Further theoretical studies found that the created DPP localized on an impurity atom in a lattice site or on the edge of the nanomaterial tip when the DP–phonon

interaction energy was sufficiently high (curve B or C in Fig. 4(b), respectively).

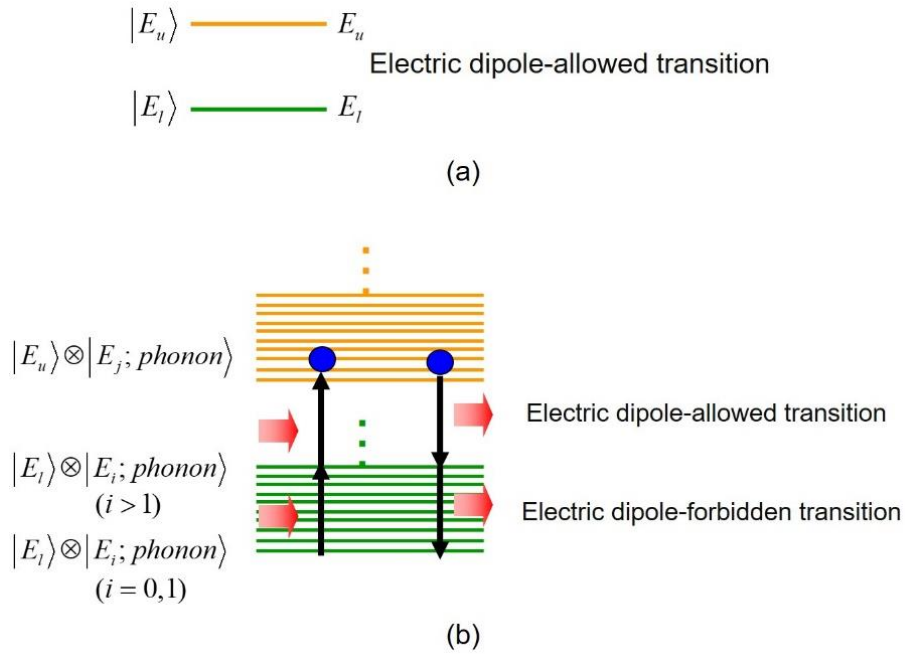

Fig. 5 Energy levels of electron and phonon.

(a) Assumed two electronic energy levels, between which the electric dipole transition is allowed. (b) Energy levels, represented by the direct product of electron and phonon energy levels. Two arrows at the left and right represent two-step excitation and de-excitation, respectively.

As a result of the theoretical studies on the DPP above, a novel light–matter interaction, named a DPP-assisted light–matter interaction, was found [28]: For simplicity, two electronic energy levels ($|E_u\rangle$ and $|E_l\rangle$) are assumed in the two nanomaterials, and an electric dipole transition is allowed between these levels (Fig. 5). It is also assumed that the photon energy $h\nu_{in}$ of the incident light is lower than the energy difference $E_d = E_u - E_l$ between the energies of these two levels. Here, by irradiating a nanomaterial 1 with incident light, the DPP is created. When another nanomaterial 2 is installed in close proximity to nanomaterial 1, the DPP energy is transferred to nanomaterial 2. Here, to describe the novel light–matter interaction between the nanomaterials 1 and 2, not only the two

electronic energy levels but also infinite numbers of phonon energy levels have to be considered. This is because the DPP is a quasi-particle in which the DP is accompanied by multi-mode coherent phonons. That is, for describing the light–matter interaction induced in nanomaterial 2 by the DPP energy transfer, the electronic energy levels in nanomaterial 2 are accompanied by an infinite number of phonon energy levels. Thus, the energy levels in nanomaterial 2 are represented by $|E_l\rangle \otimes |E_i; phonon\rangle$ and $|E_u\rangle \otimes |E_i; phonon\rangle$ $(i = 1, 2, 3, \cdots)$, where $\otimes$ is the direct product. Thus, even though $h\nu_{in} < E_d$, nanomaterial 2 can be excited to a high phonon energy level $|E_l\rangle \otimes |E_i; phonon\rangle$ $(i > 1)$ by the first arriving incident photon. Here, it should be noted that this is an electric dipole-forbidden transition because it is a transition in the electronic energy state $|E_l\rangle$. In the case where $h\nu_{in} > E_d / 2$, nanomaterial 2 is subsequently excited from $|E_l\rangle \otimes |E_i; phonon\rangle$ $(i > 1)$ to one of the phonon energy levels in the excited electronic energy level $|E_u\rangle \otimes |E_j; phonon\rangle$ by the second arriving incident photon. This transition is an electric dipole-allowed transition because it is the transition from $|E_l\rangle$ to $|E_u\rangle$. As a result of this two-step transition, a free electron is created in nanomaterial 2. The opposite transition is possible; i.e., the electron in level $|E_u\rangle \otimes |E_j; phonon\rangle$ is de-excited to $|E_l\rangle \otimes |E_i; phonon\rangle$ $(i = 0, 1)$ by the subsequent electric dipole-allowed and -forbidden transitions, and two photons are emitted. This novel DPP-assisted light–matter interaction has contributed considerably to the development of a variety of applications, as shown in Fig. 2.

3. Present status of studies on dressed photons

Recently, there have been a large number of extensive experimental studies on DPs. This section reviews the principles and practices of photon breeding (PB) devices in particular, and examples of the rapidly developing applications of these studies.

Crystalline silicon (Si) has long been a key material supporting the development of technology for more than half a century because of its numerous advantages: Si is an abundant material in the earth's crust, and is the most widely used material for modern electronics. However, because Si is an indirect-transition-type semiconductor, it has been considered to be unsuitable for light-emitting devices: Since the bottom of the conduction band and the top of the valence band in Si are at different positions in reciprocal lattice space, the momentum conservation law requires an interaction between an electron–hole pair and phonons for radiative recombination. However, the probability of this interaction is very low.

This problem has been solved by using a DPP because the phonons in the DPP can provide momentum to the conduction band electron to meet the requirement for the momentum conservation law [29]. However, the technical problem was how to fabricate such a light emitting device. To solve this problem, a novel fabrication method named DPP-assisted annealing was invented. For this annealing, an n-type Si substrate is used, in which As atoms or Sb atoms are doped. By implanting B atoms, the substrate surface is transformed to a p-type material, forming a p-n homojunction. After metallic films are coated to serve as electrodes, a forward current is injected. The principle of the DPP-assisted annealing is: By this current injection, Joule heat is generated to diffuse the B atoms. During this Joule-annealing, the substrate surface is irradiated with infrared light (for example, light with a wavelength of 1.3 μm). Because its photon energy $h\nu_{anneal}$ (=0.95eV) is sufficiently lower than the bandgap energy E_g (=1.12eV) of Si, the light can penetrate into the Si substrate without suffering absorption. Then, the light reaches the p-n homojunction to create the DPP on the B atom. The created DPP localizes at this impurity atom, as explained by curve B in Fig. 4. Then, phonons in the created DPP can provide momenta to the electron nearby to satisfy the momentum conservation law, resulting in emission of a photon. This is stimulated emission triggered by the irradiated infrared light.

The emitted light propagates away from the crystal to the outside, which means that part of the Joule energy to be used for diffusing B atoms is dissipated in the form of optical energy, resulting in local cooling that decreases the diffusion rate. As a result, by the balance between the heating by the Joule energy and the cooling by the stimulated emission, the spatial distribution of B atoms varies and reaches a stationary state autonomously.

It is expected that this DPP-assisted annealing will form the optimum spatial distribution of B atoms for efficient generation of DPPs, resulting in efficient device operation for light emission. Figure 6 shows the temporal evolution of the temperature of the device surface as the DPP-assisted annealing progressed. After the temperature rapidly rose, it fell and asymptotically approached a constant value. The features of this temporal evolution are consistent with those of the principle of the DPP-assisted annealing described above.

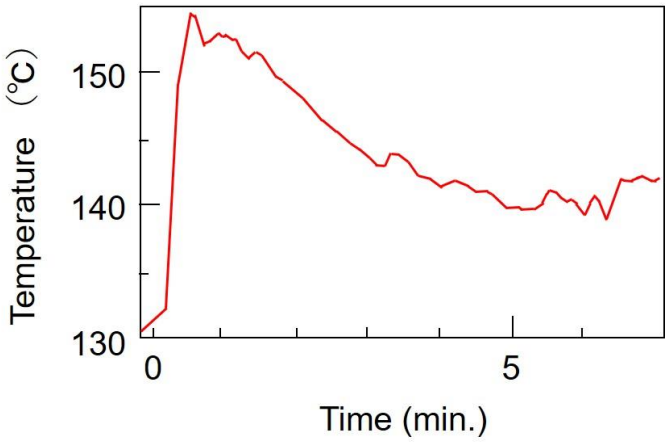

Fig. 6 Temporal evolution of the temperature of the device surface as the DPP-assisted annealing progressed.

Figure 7(a) shows a photograph of a prototype Si light emitting diode (LED) fabricated by this DPP-assisted annealing. It had an area as large as 12 mm^2. By injecting a forward current, the device emitted infrared light with a wavelength of 1.3 μm (Fig. 7(b)). The emitted optical power and the external quantum efficiency were as high as 1 W and 15% (at wavelengths in the range 1.32±0.15 μm), respectively, at room temperature. Figures 7(c) and (d) respectively show the configuration and a photograph of a recently fabricated high-power device. Its area was as small as 1 mm^2 [30]. The output power was as high 200 mW, which means that the areal power

density was three times that of the device in Figs. 7(a) and (b).

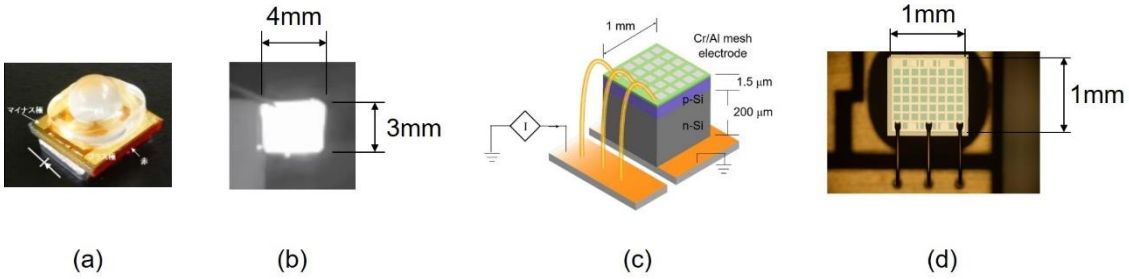

Fig. 7 Photograph of prototype Si-LED.

(a) External appearance of the fabricated device after packaging. (b) Emitted light profile. (c) and (d) show the configuration and a photograph, respectively, of the high-power device.

Figure 8 shows the light emission spectra of the fabricated Si-LED. Curves A–C are the spectra of devices fabricated by DPP-assisted annealing for 1, 7, and 30 min., respectively. They clearly show that the emitted light intensity increases with increasing DPP-assisted annealing time. The essential feature of these curves is the differences in their profiles: Although curve A has a peak around E_g, curve B shows a new peak at around 0.83 eV. In the case of curve C, no peaks were seen around E_g. Instead, a new peak appeared, identified by a downward thick arrow, at an energy that corresponds to the photon energy $h\nu_{anneal}$ of the light radiated in the DPP-assisted annealing process. This peak is evidence that DPPs were created by the light irradiation, and that the B diffusion was controlled. Other evidence is that the photon energy of the emitted light, $h\nu_{em}$, was identical to that of the irradiated light, $h\nu_{anneal}$. That is, the irradiated light served as a breeder that created a photon with energy $h\nu_{em} = h\nu_{anneal}$. For this reason, this phenomenon is named photon breeding (PB) with respect to photon energy.

Here, the separations between the energies identified by two upward thin arrows (0.83 eV and 0.89 eV) on curve C, and by the downward thick arrow (0.95 eV) were 0.06 eV, which is equal to the energy of an optical

phonon in Si. This means that the two upward thin arrows show that the DPP with an energy of 0.95 eV was converted to a free photon after emitting one and two optical phonons. This conversion process demonstrates that the light emission described here used the phonon energy levels as an intermediate state.

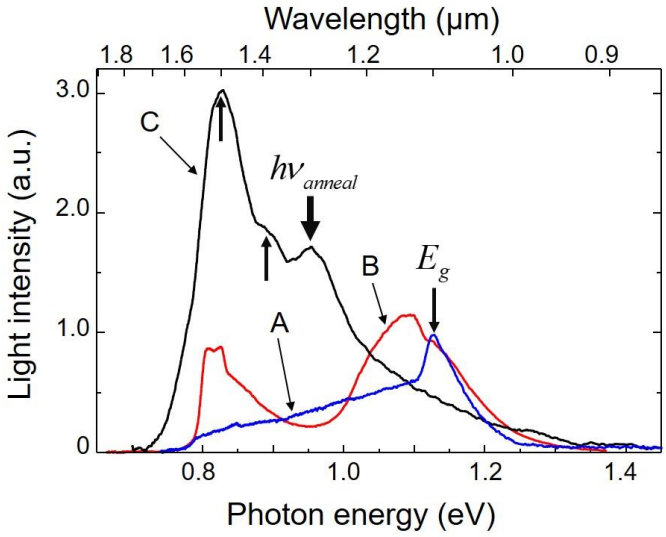

Fig. 8 Light emission spectra.

Curves A–C are the spectra of the devices fabricated by DPP-assisted annealing for 1, 7, and 30 min, respectively.

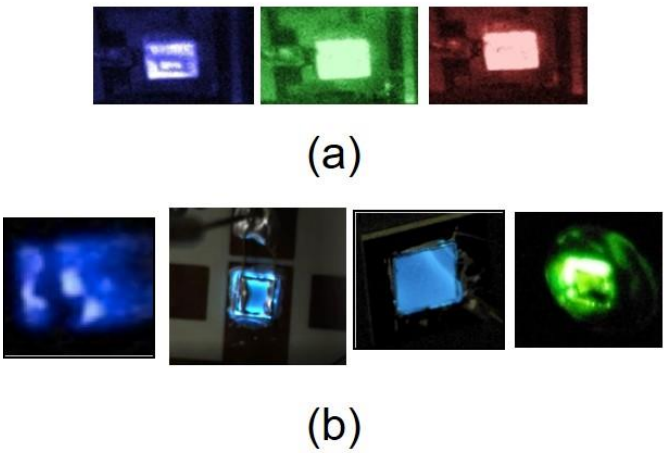

Fig. 9 Light emitted from a variety of LEDs emitting visible light.

(a) (Left to right) Blue, green, and red light emitted from Si-LEDs.

(b) (Left to right) UV-violet, bluish-white, blue, and green light emitted from SiC-LEDs.

By using the novel PB phenomenon, a variety of LEDs have been fabricated by using crystalline Si. Specifically, blue, green, and red light emitting LEDs were fabricated by radiating blue, green, and red light, respectively, during the DPP-assisted annealing (Fig. 9(a))[31]. In order to increase the efficiency of extracting this visible light, a lateral p-n homojunction structure was developed [32]. Crystalline SiC is also a known typical indirect transition-type semiconductor. A variety of visible LEDs have been fabricated even using this material. They were fabricated by irradiating them with UV-violet, bluish-white, blue, and green light during the DPP-assisted annealing, and respectively emitted UV-violet, bluish-white, blue, and green light (Fig. 9(b))[33-36].

PB was observed not only with respect to photon energy but also with respect to photon spin. That is, the polarization of the emitted light was equivalent to that of the light irradiated during the DPP-assisted annealing (Fig. 10)[37].

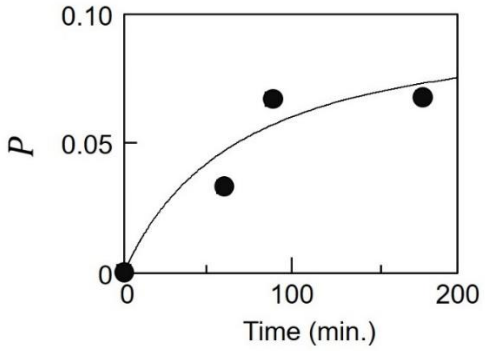

Fig. 10 Relation between the DPP-assisted annealing time and the degree of polarization $P=\left(I_{\parallel}-I_{\perp}\right)/\left(I_{\parallel}+I_{\perp}\right)$ of the light emitted from the Si-LED. $I_{\parallel}$ and $I_{\perp}$ are the light intensities emitted from the Si-LED whose polarizations are parallel and perpendicular to that of the light irradiated during the DPP-assisted annealing, respectively.

The origin of the PB was attributed to the spatial distribution of B atoms, which was controlled autonomously during the DPP-assisted annealing. By analyzing the three-dimensional spatial distribution of B atoms at the p-n homojunction, acquired by atom probe field ion microscopy with sub-nanometer resolution, it was found that the B atoms were apt to orient along a plane parallel to the top surface of the Si crystal and to form

pairs with a length $d = 3a$, where a (=0.54 nm) is the lattice constant of the Si crystal.

As a preliminary discussion on this origin, Fig. 11 shows the calculated vibration amplitudes of the crystal lattice of Si atoms, where a one-dimensional lattice was assumed for simplicity [27]. The curve A shows the amplitude of the lattice vibration in the case where the lattice is formed only by the Si atoms, which corresponds to a non-localized phonon mode. On the other hand, when some of the Si atoms are replaced by impurity B atoms, the amplitude profile of the lattice vibration changes greatly. As represented by curves B and C, the vibration amplitude is localized at the B atom-pair, because the B atom-pair serves as a cavity resonator to confine the lattice vibration. The confined lattice vibration corresponds to the localized phonon mode. As a result, impurity B atom-pairs serve as phonon localization centers, at which the DPPs can be created and localized efficiently.

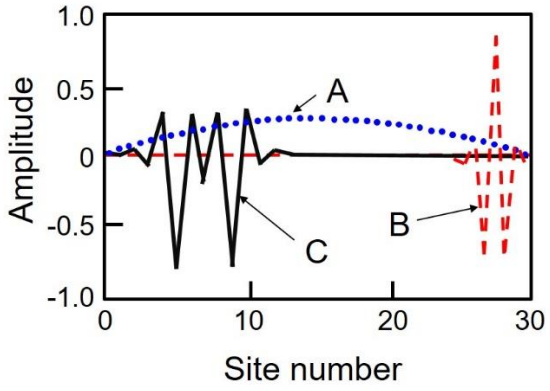

Fig. 11 Vibration amplitudes of the crystal lattice of Si atoms.
The number of lattice sites is 30. Curve A represents the non-localized mode. Curves B and C represent the first and second localized modes, respectively, where impurity atoms were assumed to be at sites 5, 9, 18, 25, 26, and 27.

The main discussion below follows from the preliminary discussion above: If d is equal to the lattice constant a, the B atom-pair can orient in a direction parallel to the [1,0,0], [0,1,0], or [0,0,1] orientation because the Si crystal is composed of multiple cubic lattices. As a result, the momentum of the localized phonon points in this direction, which corresponds to the $\Gamma - X$ direction in reciprocal space (Fig. 12(a)). Thus, a photon is efficiently emitted because this $\Gamma - X$ direction is the same as the direction of the momentum of the phonon required for recombination between an electron at

the bottom of the conduction band at the X-point and a hole at the top of the valence band at the Γ-point. Here, it should be noted that the value of the momentum of the phonon has to be h/a for this electron–hole recombination to take place. Furthermore, it should also be noted that the value of the momentum of the mode localized at the B atom-pair with $d=3a$ is $h/3a$. By comparing these two values, it is found that the DPP at this B atom-pair has to create three phonons for recombination. In the other words, the B atom-pairs with $d=3a$ most efficiently create three phonons for light emission. As a result, as is schematically shown in Fig. 12(b), the emitted photon energy $h\nu_{em}$ is expressed as $h\nu_{em}=E_g-3E_{phonon}$. By substituting the values of E_g (= 1.12eV) and the relevant optical mode phonon energy E_{phonon} (=65meV) into this equation, the value of $h\nu_{em}$ is derived to be 0.93 eV, which is nearly equal to the photon energy $h\nu_{anneal}$ (=0.95eV) irradiated during the DPP-assisted annealing. This numerical relation confirms that PB with respect to photon energy occurs.

In the case where the Si crystal surface is irradiated with linearly polarized light during the DPP-assisted annealing, analyses of the spatial distribution of B atoms confirmed that B atom-pairs with $d=3a$ were also apt to be formed, and the direction of the B atom-pairs was normal to the polarization direction of the irradiated light. A possible origin of the induced polarization of the emitted light is as follows: First, when the Si-LED is fabricated by the DPP-assisted annealing, transverse optical phonons are created at the B atom-pairs and couple with the DPs. The vibration direction of these phonons is parallel to that of the electric field of the polarized light irradiated during the DPP-assisted annealing. Next, when the fabricated LED is operated, since these phonons are created again, the direction of the electric field vector of the emitted light becomes also parallel to the vibration direction of these phonons. Therefore, the polarization direction of the emitted light becomes identical to that of the light irradiated during the DPP-assisted annealing.

In summary, the spatial distribution of B atoms was controlled autonomously by the DPP-assisted annealing to satisfy the momentum

conservation law and to realize PB with respect to photon energy and to photon spin.

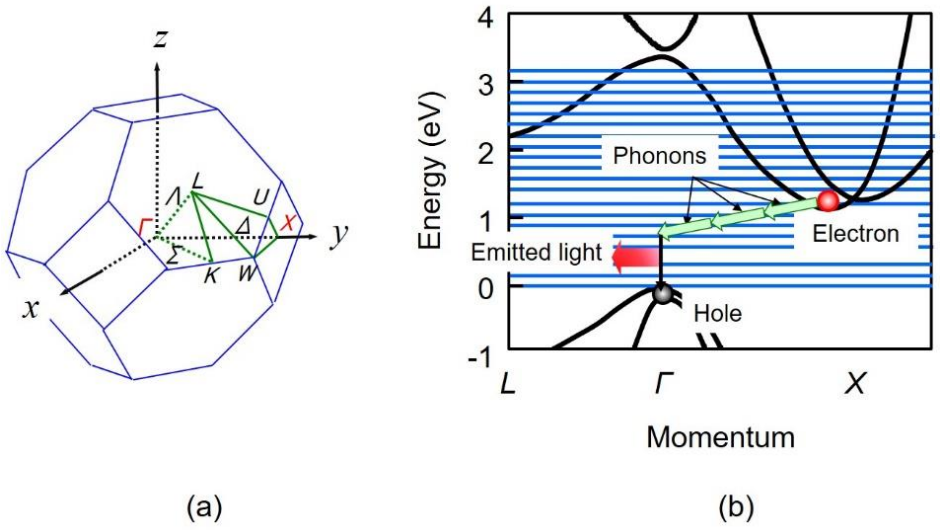

Fig. 12 Energy band structure of Si.

(a) A unit cell of the Si crystal in reciprocal lattice space. (b) Energy band structure and schematic illustration of light emission. Blue horizontal lines represent phonon energy levels involved in the light emission.

Si-lasers were also fabricated by using the DPP-assisted annealing. Figure 13(a) shows the device structure and a scanning electron microscopic image of the fabricated device [38]. A simple ridge waveguide was incorporated into the structure, and the cleaved facets were used as mirrors of a Fabry-Perot cavity. DPP-assisted annealing was then carried out by injecting 1.3 μm-wavelength light into the cavity through one of the end facets. Figures 13(b) and (c) show the light emission spectra of the fabricated Si-laser. Above the threshold, a sharp lasing spectrum was observed (Fig. 13(b)), which demonstrates single-mode oscillation at room temperature even though the cavity length was as long as 550 μm. The origin of this single-mode oscillation is that the low infrared absorption by the Si provides a low threshold for the principal longitudinal mode at the optical amplification gain spectral peak and, as a result, the gains for other modes are depleted by this principal mode due to nonlinear mode competition [39,40]. The spectral profile below the threshold (Fig.13(c)) does not show any ASE spectra, which is evidence of the gain depletion due to the mode

competition above.

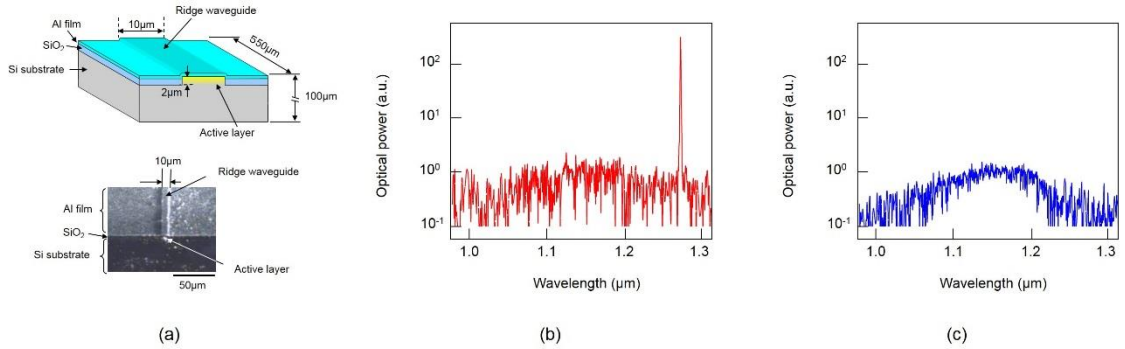

Fig. 13 Structure of Si laser and the light emission spectra.

(a) Structure and a scanning electron microscopic image of the device. (b),(c) Spectral profiles above and below the threshold, respectively.

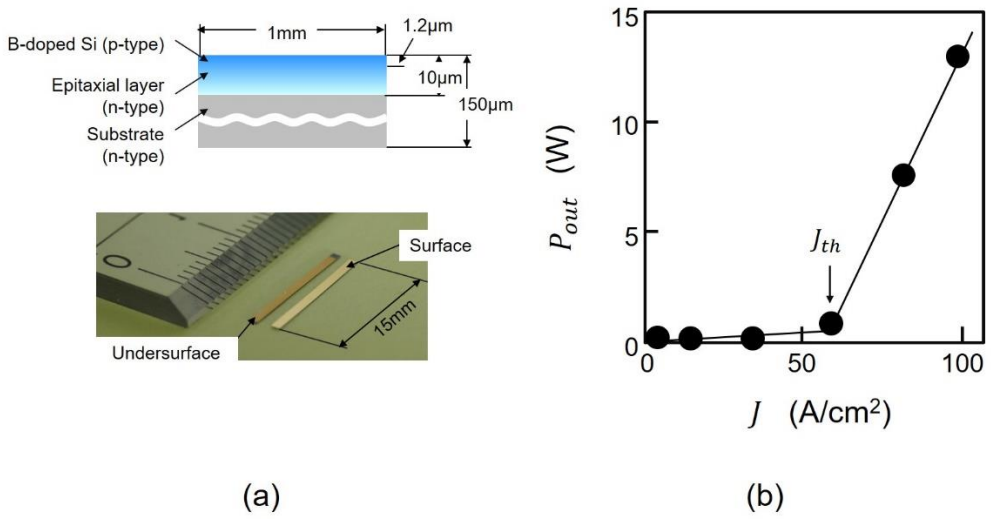

Fig. 14 Structure of a high-power Si laser and the output power.

(a) Structure and a photograph of the device. (b) Relation between the injected current density and the output optical power.

By modifying the device structure in Fig. 13(a), a high-power infrared laser device was successfully fabricated by utilizing the very low infrared absorption of crystalline Si. Figure 14(a) shows a photograph of the device [41]. A cross-sectional profile is also shown, in which the ridge waveguide was not built-in because very efficient optical confinement was not expected by this waveguide as long as the device had a p-n homojunction. Instead, the cavity length was increased to 15 mm to realize high power. After the

DPP-assisted annealing, the relation between the injected current density J and the output power P_{out} of the fabricated laser device was measured. As shown in Fig. 14(b), an output power as high as 13 W was obtained. This value was more than 10^3-times that of a conventional double heterojunction-structured InGaAsP/InP laser (10 mW at 1.3 μ m wavelength: SLT1130 series manufactured by Sumitomo Electric). The threshold current density J_{th} was as low as 60 A/cm^2.

Since crystalline Si was used without a built-in waveguide, the structure of the present device is more similar to those of solid-state and gas lasers than those of conventional double heterojunction-structured semiconductor lasers [42,43]. Further similarities can be found by referring to the magnitude of the absorption loss: In the case of solid-state and gas lasers, electronic transitions in electronically isolated ions, atoms, and molecules are used for lasing. Therefore, even though direct electric current injection to these laser media is difficult, the absorption loss per unit volume is very low. Thus, a high optical output power can be obtained by increasing the size of the laser medium even though the photon density of the lasing light was low

Since the DPPs used in the present Si laser were electronically isolated, as in the case of ions in the solid-state and gas lasers above, the absorption loss per unit volume was maintained very low. Thus, the threshold current density was very low. Furthermore, the optical output power was greatly increased by increasing the size of the Si crystal even though the photon density of the lasing light was low. An additional advantage was that electrons could be easily supplied by direct electric current injection, due to the low recombination loss in the crystalline Si.

For comparison, in the case of conventional semiconductor lasers, coupled electrons and holes in the conduction and valence bands, respectively, have been used for lasing. Therefore, direct electric current injection to the laser medium is easy. An additional advantage is that the laser medium can be very small. However, the problem was that the absorption loss per unit volume was large, making it impossible to achieve high optical output power and low threshold current density even though the photon density of the lasing light was high.

It has been believed for a long time that indirect transition-type semiconductors are unsuitable for use as laser media. Instead, direct transition-type semiconductors have been widely used until now [44]. However, thanks to the advent of DP science and technology, DPPs have resulted in the manifestation of large optical amplification gain in indirect transition-type semiconductors, which was the secret to the dramatically high optical output power and low threshold current density realized by using crystalline Si.

4. Future outlook

After extensive experimental and theoretical studies on DPs in the last three decades, the main effort in recent years has focused on experimental studies, and the development of generic technologies. To achieve further advances, now is a good opportunity to promote novel theoretical studies.

It should be pointed out that the theoretical studies carried out so far relied on nanomaterial structures, i.e., on the structures of electron energy levels and phonon energy levels. In order to draw more generic physical pictures, new routes to future theoretical studies should not strongly rely on such detailed material structures. Such routes are expected to be developed by the following three steps:

Step 1: To draw a more generic and basic physical picture of the DP.

Step 2: To draw a picture that allows us to treat multiple DPs created in a macroscopic material.

Step 3: To draw a picture for demonstrating how to take out the DP from a nano-system to a macro-system.

A hint to achieving step 1 can be found in the photon dispersion relation, i.e., the relation between the momentum and energy of a photon, as shown in Fig. 15. Since conventional optics deals with propagating light (free photons with a definite electromagnetic mode), its dispersion relation is represented by the black curve in this figure when the photon exists in a macroscopic material. The three-dimensional profile of this curve is a shell. The profile in vacuum is represented by the blue line, whose three-dimensional profile is a so-called light cone, which is a special case of the shell. That is, a free photon exists on the shell, and because of this, conventional optics can be called *on-shell science*.

In the case of a DP, on the contrary, it should be noted that its electromagnetic mode cannot be defined because of its nanometric nature, which makes the use of the dispersion relation invalid. This means that the DP does not exist on the shell. Instead, it exists off the shell, a situation that is represented by the shaded green rectangle in this figure. Intrinsic features of the off-shell photon are: Since the momentum uncertainty Δp, represented by the horizontal double-headed arrow in this figure, is large, the size of the field Δx is small, which is a consequence of the uncertainty principle $\Delta p \cdot \Delta x \geq \hbar$. Because of this feature, the DP has been called an optical near field. Furthermore, since the energy uncertainty ΔE, represented by the vertical double-headed arrow in this figure, is also large, the duration of the created photon Δt is short, which is also a consequence of the uncertainty principle $\Delta E \cdot \Delta t \geq \hbar$. A photon with this feature has been called a virtual photon. From these two intrinsic features, it is found that the off-shell photon is an optical near field and a virtual photon, which is the physical picture of the DP.

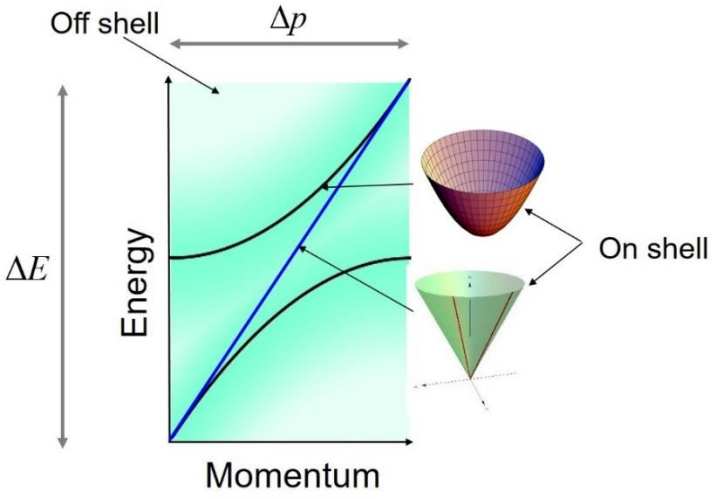

Fig. 15 Dispersion relation.

Two black curves represent the relation of a photon in a macroscopic material. The blue line is for a photon in free space. The green shaded rectangle represents that for the dressed photon. The brown and green three-dimensional forms represent a shell and a light cone, respectively.

With the help of this hint, realization of step 1 was promoted by novel theoretical analysis of the Clebsch-dual electromagnetic field, for which a

notion of a space-time vortex field was used [45,46]. The main results of this analysis are: (1) It was found that the DP exists in a spacelike domain of the Riemannian manifold. (2) The spatial profile of the DP is represented by the Yukawa function, which is equivalent to eq. (8). Furthermore, it was found that the effective mass m_{eff} of the DP field, being inversely proportional to the size a of localization (a consequence of the Klein-Gordon's equation), is expressed as $m_{eff} = \sqrt{E^2 - \chi^2}$. Here, E and χ are the instantaneous energy spent to create the DP and a characteristic scale of the nanomaterial, respectively. It suggests that the DP can be transferred from the spacelike to the timelike domain if $E > \chi$, and that the DP can be transformed to be observable, however, within the very short duration Δt above. (3) It was found that the energy-momentum tensor of the DP became isomorphic to Einstein's equation, which implies that the DP is closely related to the vacuum energy.

The reasons why step 2 is indispensable are: As was reviewed in the previous section describing the DPP-assisted annealing of crystalline Si, there were too many Si atoms, electrons, B atoms, DPs, and DPPs in the crystal. Since it is difficult to treat these multiple quasi-particles and elementary particles by the conventional deterministic method of theoretical analysis, a method of avoiding this difficulty was proposed by considering a system composed of these mutually interacting particles as a complex system [47].

Based on this consideration, computer simulations were carried out by using a stochastic model. Here, an interactive random-walk process on a crystal lattice and phenomenological coupled-Poisson process were assumed to describe the diffusive motion of doped B atoms and electron–phonon coupling, respectively. As a result, the main experimental results were successfully reproduced, such as the temporal behaviors of the crystal temperature and the emitted light intensity observed during the DPP-assisted annealing.

Step 3 is indispensable, especially for connecting the theoretical and experimental studies. In the experiment, it is essential to create or detect the DP in the most efficient manner; that is to say, the most efficient micro–macro conversion is required. To meet this requirement, high-quality fiber

probe tips (Fig. 1) have been developed [6] in order to create or detect DPs with high spatial resolution or high sensitivity. The concept of micro–macro duality in the quantum field has been found to be a powerful and promising theoretical tool for drawing a picture of the micro–macro conversion [48], and detailed studies have commenced [49].

In order to support further progress in achieving steps 1-3 above, another route to future theoretical studies is also under development, based on the classical electromagnetic field theory [50,51]. These studies recently found that the longitudinal electric field, which has been ignored in conventional optics, induced a non-resonant light–matter interaction in a nanometric space, as has been previously observed in several experiments [52].

Figure 16 represents a variety of phenomena occurring in nature, which have similar features to those of the DP. They have been found in nano-systems and in macro-systems, as well as in organic materials and in inorganic materials. In an inorganic nano-system, a representative example is a meson, which connects two nucleons. Some features of the meson are similar to those of the DP, which connects nanomaterials by means of DP energy exchange. It has been known that the potential profile of the meson is expressed by the Yukawa function, shown in eq. (8).

In an organic nano-system, an example is a light-harvesting photosynthetic system, whose light trapping operation is similar to the operation of logic gate devices based on DP energy transfer [53]. In an organic macro-system, an example is the natural computing observed in single-celled amoeboid organisms [54], whose signal transmission features are similar to those of DP energy transfer. Some features of this computing have been demonstrated by using the logic gate devices described above [55].

Finally, one example of an inorganic macro-system is the photochemical reaction in the weathering of rocks. Some features of this reaction are similar to the photochemical reaction induced by a DP, which has been used for polishing material surfaces to atomic-level flatness [56]. Another example is a binary pulsar [57]. Some of the features of the gravitational wave radiation from a binary pulsar are similar to the propagating light radiation from two nanomaterials as a result of DP energy exchange and relaxation.

By referring to Fig. 16, it can be understood that the DP is not a

special topic of a narrow field of science but is connected to more general and broader scientific fields.

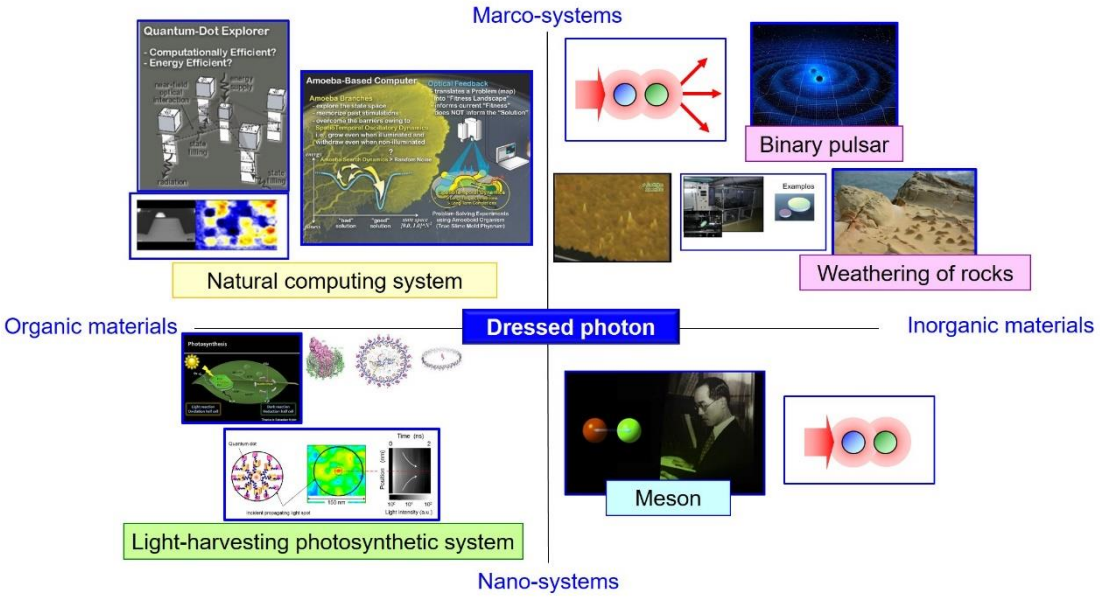

Fig. 16 A variety of phenomena occurring in nature that have similar features to those of the dressed photon.

5. Conclusion

The present paper reviewed some of the experimental and theoretical studies on DPs carried out in the last three decades. It was pointed out that the main effort in recent years has focused on experimental studies, resulting in the development of generic technologies for supporting modern society. By referring to these drastic experimental advances, it was also pointed out that further effort should be devoted to finding new routes to theoretical studies from now on, by which a more detailed and precise physical picture of the DP can be drawn, and also to establish criteria for novel application systems. That is, now comes a good opportunity to take a step toward a novel generic science by promoting theoretical studies on DPs.

The routes to this novel science can be developed by following the three steps reviewed in the last section. It is expected that a novel process for creating or detecting DPs will be found by using these developed theories as criteria for designing novel experimental systems, resulting in further advances in DP science and establishing a generic off-shell science in the

near future. Future advances in these studies are expected to be reported in forthcoming papers to be published in this Off-shell archive in the near future.

Acknowledgements

The author acknowledges Drs. I. Ojima and H. Sakuma (Research Origin for Dressed Photon), Dr. H. Saigo (Nagahama Bio Univ.), Dr. K. Okamura (Nagoya Univ.), Dr. I. Banno (Yamanashi Univ.), and Dr. S. Sangu (Ricoh Company, Ltd.) for their collaboration in theoretical studies on dressed photons. These theoretical studies were partially supported by Nichia Corp..

References

[1] E.H.Synge: "A Suggested Method for Extending Microscopic Resolution into the Ultra-Microscopic Region," Phil. Mag., **6** (1928) pp.356-362.

[2] H. Bethe: "Theory of diffractin by small holes," Phys. Rev., **66** (1944) pp.163-182.

[3] C.J. Bouwkamp: " On the Diffraction of Electro-Magnetic Waves by Small Circular Discs and Holes," Philips Res. Rep., **5** (1950) pp.401-422.

[4] E. A. Ash and G. Nicholls:" Super-Resolution Aperture Scanning Microscope," Nature, **237** (1972) pp.510-516.

[5] D.W. Pohl and D.Courjon (ed.): *Near Field Optics* (Kluwer, Dordrecht, 1993) pp.1-324.

[6] M. Ohtsu(ed.): *Near-Field Nano/Atom Optics and Technol.* (Springer, Tokyo, 1998) pp.31-100.

[7] M. Ohtsu(ed.): *Near-Field Nano/Atom Optics and Technol.* (Springer, Tokyo, 1998) pp.101-152.

[8] For example, JASCO catalogue for Scanning Near-Field Optical Microspectrometer (NFS series), (JASCO, Tokyo, 2003).

[9] Optical Society of Japan (organizer): *The 14th International Conference on Near-Field Optics, Nanophotonics, and Related Technologies*, Shizuoka, Japan, Sept.4-8, 2016.

[10] Condensed Matter Res. Inst., Seoul National Univ. (organizer): *The First Asia-Pacific Workshop on Near Field Optics*, Seoul, Korea, Aug. 17-18, 1996.

[11] National Chung-Kung Univ.(organizer): *The 11th Asia-Pacific Conference on Near-Field Optics*, Tainan, Taiwan, July 10-13, 2017.

[12] M. Ohtsu: *Dressed Photons* (Springer, Heidelberg, 2014) pp.1-324.

[13] M. Ohtsu: *Dressed Photons* (Springer, Heidelberg, 2014) pp.89-214.

[14] T. Kawazoe, T. Takahashi, and M. Ohtsu: "Evaluation of the dynamic range and spatial

resolution of nonadiabatic optical near-field lithography through fabrication of Fresnel zone plates," Appl. Phys.B, **98** (2010) pp.5-11.
[15] T. Matsumoto, K. Nakamura, T. Nishida, H. Hieda, A. Kikitsu, K. Naito, and T. Koda: "Thermally assisted magnetic recording on a bit-patterned magnetic medium using a near-field optical head with a beaked metallic plate," Proc. ISOM'07 (2007) pp.90-91.
[16] T. Yatsui, W. Nomura, M. Naruse, and M. Ohtsu: "Realization of an atomically flat surface of diamond using dressed photon-phonon etching," J. Phys.D, **45** (2012) 475302.
[17] M. Ohtsu: "Silicon Light Emitting Diodes and Lasers Using Dressed Photons," Prog. in Nanophotonics 3 (ed. M. Ohtsu) (Springer, Heidelberg, 2015) pp.1-56.
[18] M. Ohtsu: *Dressed Photons* (Springer, Heidelberg, 2014) pp.89-136.
[19] M. Naruse, T. Miyazaki, T. Kawazoe, K. Kobayashi, S. Sangu, F. Kubota, and M. Ohtsu: "Nanophotonic computing based on optical near-field interactions between quantum dots," IEICE Trans. Electron., **E88-C** (2005) p.1817-1823.
[20] H. Fujiwara, T. Kawazoe, and M. Ohtsu: "Nonadiabatic nongenerated excitation by optical near-field and its application to optical pulse-shape measurement," Appl. Phys.B, **100** (2010) pp.85-91.
[21] M. Naruse, M. Aono, S.-J. Kim, T. Kawazoe, W. Nomura, H. Hori, M. Hara, and M. Ohtsu: "Spatiotemporal dynamics in optical energy transfer on the nanoscale and its application to constraint satisfaction problems," Phys. Rev. B, **86** (2012) 125407.
[22] T. Kawazoe, H. Fujiwara, K. Kobayashi, M. Ohtsu: "Visible light emission from dye molecular grains via infrared excitation based on the nonadiabatic transision induced by the optical near field," IEEE J. Select. Top. on Quantum Electron., **15** (2009)pp.1380-1386.
[23] N. Tate, Y. Liu, T. Kawazoe, M. Naruse, T. Yatsui, and M. Ohtsu: "Fixed-distance coupling and encapsulation heterogeneous quantum dots using phonon-assisted photo-curing,"Appl. Phys.B, **110** (2013) pp.39-45.
[24] M. Ohtsu: *Dressed Photons* (Springer, Heidelberg, 2014) p.3.
[25] M. Ohtsu: *Dressed Photons* (Springer, Heidelberg, 2014) p.31.
[26] M. Ohtsu: *Dressed Photons* (Springer, Heidelberg, 2014) pp.33-36.
[27] K. Kobayashi, Y. Tanaka, T. Kawazoe, and M. Ohtsu: "Localized Photon Inducing Phonons' Degrees of Freedom," Prog. in Nano-Electro-Optics VI (ed. M. Ohtsu) (Springer, Heidelberg, 2008) pp.41-66.
[28] K. Kobayashi, S. Sangu, H. Ito, and M. Ohtsu: "Near-field optical potential for a neural atom," Phys. Rev.A, **63** (2001) 013806.
[29] T. Kawazoe, M.A. Mueed, and M. Ohtsu: "Highly efficient and broadband Si homojunction structured near-infrared light emitting diodes based on the phonon-assisted optical near-field process," Appl. Phys.B, 104 (2011) pp.747-754.

[30] B. Thubthimthong, T. Kawazoe, and M. Ohtsu: "*Spectral Analysis of a High-Power Infrared Silicon Light Emitting Diode of Dressed Photons*," Abstracts of the OSA Laser Congress, October 1-5, 2017, Nagoya, Japan, paper number JTh2A.10.

[31] M. A. Tran, T. Kawazoe, and M. Ohtsu: "Fabrication of a bulk silicon p-n homojunction-structured light emitting diode showing visible electroluminescence at room temperature," Appl. Phys. A, **115** (2014) pp.105-111.

[32] M. Yamaguchi, T. Kawazoe, T. Yatsui, and M. Ohtsu: "Spectral properties of a lateral p-n homojunction-structured visible silicon light-emitting diode fabricated by dressed-photon—phonon-assisted annealing," Appl. Phys.A, **121** (2015) 1389-1394.

[33] T. Kawazoe, M. Ohtsu: "Bulk crystal SiC blue LED with p-n homojunction structure fabricated by dressed-photon—phonon-assisted annealing," Appl. Phys. **A 115** (2014) pp.127-133.

[34] K. Suzuki, K. Chieda, T. Kawazoe, T. Yatsui, and M. Ohtsu : "*Control of emission spectrum from a green SiC-LED using dressed-photon—phonon annealing*," Abstract of the 61st JSAP Spring Meeting, March 2014, Sagamihara, Japan, paper number 18a-F12-11.

[35] Q.H. Vo, T. Kawazoe, and M. Ohtsu: "*Fabrication of SiC-LED using d dressed-photon—phonon annealing with two light sources*," Abstract of the 61st JSAP Spring Meeting, March 2014, Sagamihara, Japan, paper number 18a-F12-10.

[36] T.Kawazoe, K. Nishioka, M. Ohtsu : "SiC light emitting diode and its polarization control using dressed photons," Abstract of the International Display Workshop 2014, (Niigata, Japan, Dec., 2014) pp.1061-1063.

[37] T. Kawazoe, K. Nishioka, and M. Ohtsu: "Polarization control of an infrared silicon light-emitting diode by dressed photons and analyses of spatial distribution of doped boron atoms," Appl. Phys. A, 121 (2015) pp.1409-1415.

[38] T. Kawazoe, M. Ohtsu, K. Akahane, and N. Yamamoto: "Si homojunction structured near-infrared laser based on a phonon-assisted process," Appl. Phys. B, 107 (2012) pp.659-663.

[39] M. Ohtsu, Y. Teramachi, and T. Miyazaki: "Mode Stability Analysis of Nearly Single-Longitudinal-Mode Semiconductor Lasers," IEEE J. Quantum Electron., 24 (1988) pp.716-723.

[40] M. Ohtsu and Y. Teramachi: "Analyses of Mode Partition and Mode Hopping in Semiconductor Lasers," IEEE J. Quantum Electron., **25** (1989) pp.31-38.

[41] T. Kawazoe, K. Hashimoto, and S. Sugiura: "High-power current-injection type Silicon Laser using nanophotonics," Abstract of the EMN Nanocrystals Meeting, Oct. 2016, X'ian, China, pp.9-11.

[42] M. Ohtsu, *Coherent Quanatum Optics and Technology*, Tokyo, Dordrecht, Boston,

London: KTK Scientific and Kluwer Academic, 1992, pp.49-81.
[43] M. Ohtsu, *Highly Coherent Semiconductor Lasers*, Boston, London: Artech House, 1992, pp.7-60.
[44] W.P. Dumke: "*Interband Transitions and Maser Action*," Phys. Rev., **127** (1962) 1559-1563.
[45] H. Sakuma, I. Ojima, and M. Ohtsu: "Dressed Photons in a New Paradigm of Off-shell Quantum Fields," J. Quantum Electron., in press.
[46] H. Sakuma, I. Ojima, and M. Ohtsu: "Novel View Towards Gauge Condition as a Conceptual Basis of Dressed Photons," Abstracts of the 11th Asia-Pacific Conference on Near-Field Optics, July, 2017 , Tainan, Taiwan, p.32.
[47] M. Katori and H. Kobayashi: "Nonequilibrium Statistical Mechanical Models for Photon Breeding Processes Assisted by Dressed-Photon-Phonons," *Prog. in Nanophotonics* 4 (ed. M. Ohtsu and T. Yatsui) (Springer, Heidelberg, 2017) pp.19-55.
[48] I. Ojima: "Micro-macro duality in quantum physics,"
in *Stochastic Analysis: Classical and Quantum Perspective of White Noise Theory*, T. Hida (ed.) (World Scientific, 2005) pp. 143-161.
[49] M. Ohtsu, I. Ojima, and H. Saigo: "Who Has Seen A Free Photon? ---From Mathematical Physics to Light-Matter Fusion Technologies---," Abstracts of the 11th Asia-Pacific Conference on Near-Field Optics, July 10-13, 2017, Tainan, Taiwan, p.54.
[50] I. Banno and M. Ohtsu, "Irrationality of the Permittivity in Non-resonant Near-field Optics", Abstracts of the 11th Asia-Pacific Conference on Near-Field Optics, July 10-13, 2017, Tainan, Taiwan, p.35.
[51] I. Banno and M. Ohtsu, "The Nonlinear Response Theory for Near-field Optics and Application to Non-resonant Effect", Abstracts of the 11th Asia-Pacific Conference on Near-Field Optics, July 10-13, 2017, Tainan, Taiwan, p.62.
[52] M. Ohtsu: *Dressed Photons* (Springer, Heidelberg, 2014) pp.137-214.
[53] M. Ohtsu: T. Kawazoe, K. Kobayashi, and M. Ohtsu, "Optical nanofountain: A biomimetic device that concentrates optical energy in a nanometric region," Appl. Phys. Lett., **86** (2005) 103102.
[54] M. Aono, S.-J. Kim, M. Naruse, M. Wakabayashi, H. Hori, M. Ohtsu, and M. Hara: "Amoeba-Inspired Nanoarchtectonic Computing: Solving Intractable Computational Problems Using Nanoscale Photoexcitation Transfer Dynamics," Langmuir, **29** (2013) pp.7557-7564.
[55] M. Naruse, W. Nomura, M. Aono, M. Ohtsu, Y. Sonnenfraud, A. Drezet, S. Huant, and S.-J. Kim: "Decision making based on optical excitation transfer via near-field interactions between quantum dots," J. Appl. Phys., **116** (2014) 154303.

[56] M. Ohtsu: *Dressed Photons* (Springer, Heidelberg, 2014) pp.160-169.
[57] R.W. Hilditch: *An Introduction to Close Binary Stars* (Cambridge University Press, 2001).